

ZIF-Derived Hierarchically Porous Fe-Zn-N-C Catalyst Synthesized via a Two-Stage Pyrolysis for Highly Efficient Oxygen Reduction Reaction in Both Acidic and Alkaline Media

Experimental Section

Reagents

Tris(acetylacetonato)iron(III) ($\text{Fe}(\text{acac})_3$, 98%), 2-methylimidazole (98%), KOH (95%) and HClO_4 (70%) were purchased from Shanghai Aladdin Bio-Chem Technology Co., Ltd. Zinc nitrate hexahydrate ($\text{Zn}(\text{NO}_3)_2 \cdot 6\text{H}_2\text{O}$, 98%), H_2SO_4 (98%), methanol (99.7%) and N, N-dimethylformamide (DMF, 99.5%) were purchased from Sinopharm Chemical Reagent Co., Ltd. Nafion D-520 dispersion (5% w/w in water and 1-propanol, DuPont) and commercial Pt/C catalyst (20 wt%, Johnson Matthey, JM) were purchased from Shanghai Hesen Electronic Device Co., Ltd. All the chemicals and reagents were used without any further purification. The ultrapure water (18.2 M Ω cm) was used for solution preparation in all experiments.

Synthesis of Fe-Zn-ZIF

Typically, $\text{Fe}(\text{acac})_3$ (0.4 mmol) and $\text{Zn}(\text{NO}_3)_2 \cdot 6\text{H}_2\text{O}$ (4 mmol) were dissolved in 45 mL of methanol to form a clear solution in flask A. 2-methylimidazole (15.8 mmol) was dissolved in 10 mL of methanol in flask B, which was subsequently added into flask A and ultrasonicated for 10 min and then vigorously stirred for 1 h at room temperature. The resultant solution was transferred into a Teflon-lined stainless-steel autoclave (100 mL) and heated at 120 °C for 4 h. The resultant product was separated by centrifugation and washed alternately with DMF and methanol each for three times, and finally dried at 70 °C under vacuum for overnight.

Two-stage pyrolysis of Fe-Zn-ZIF

The powder of Fe-Zn-ZIF was transferred into a corundum boat and placed in a tube furnace, which was heated to 400 °C with a heating rate of 5 °C min⁻¹ and held at this temperature for 1 h, and then it was heated to the desirable temperature (800 900 or 1000 °C) with a heating rate of 1 °C min⁻¹ and held at that temperature for 2 h under flowing N_2 , followed by cooling to room temperature. The obtained sample was stirred in 0.5 M H_2SO_4 solution at 80 °C for 7 h, and then washed and dried, and the resultant sample was heated to 900 °C with a heating rate of 5 °C min⁻¹ and kept at that temperature for 2 h under flowing N_2 , followed by cooling to room temperature. The finally obtained sample was denoted as Fe-Zn-N-C-900-2 (Fe-Zn-N-C-800-2 or Fe-Zn-N-C-1000-2).

One-stage pyrolysis of Fe-Zn-ZIF

The Fe-Zn-ZIF sample was heated to 900 °C with a heating rate of 5 °C min⁻¹ and kept at 900 °C for 3 h under flowing N_2 and then naturally cooled to room temperature. The other procedures used were the same as those used in the two-stage pyrolysis process. The finally obtained sample was denoted as Fe-Zn-N-C-900-1.

Physical characterization

The morphology, structure and composition of the synthesized materials were characterized by HRTEM (JEM-2100F, JEOL), XRD (D8 Advance, Bruker), XPS (VG Multilab 2000, Bruker), surface area and porosity analyzer (ASAP2460,

Micromeritics) and laser confocal micro-Raman spectroscopy (DXR, American Thermo Electron).

Electrochemical characterization

Electrochemical measurements were carried out by using an electrochemical workstation (PGSTAT 302 N, Metrohm Autolab) in a three-electrode system consisting of a graphite rod counter electrode, a calibrated reference electrode (Ag/AgCl for acidic electrolyte and Hg/HgO for alkaline electrolyte), and a catalyst-modified glassy-carbon (GC) working electrode. All the electrode potentials reported in this work were reported with respect to RHE. The loading of Fe-Zn-N-C sample on the GC electrode was $642 \mu\text{g}\cdot\text{cm}^{-2}$ and the loading of the commercial Pt/C (20 wt. %, Johnson Matthey) catalyst on GC electrode was $86 \mu\text{g}\cdot\text{cm}^{-2}$. The temperature of electrolyte (0.1 M HClO₄ or 0.1 M KOH) was maintained at 25 °C with circulating ethylene glycol/water. The ORR performance of the catalyst was measured in O₂-saturated electrolyte by LSV with a sweep rate of 10 mV s⁻¹ at 1600 rpm. The H₂O₂/HO₂⁻ yield (η) and the electron transfer number (n) during ORR were determined by using RRDE (Pine) technique with the Pt ring potential set to 1.2 V vs. RHE (Equations 1 and 2).

$$\eta = 200 \frac{I_r / N}{I_d + I_r / N} \quad (1)$$

$$n = 4 \frac{I_d}{I_d + I_r / N} \quad (2)$$

where I_r is the ring current, I_d is the disk current, and N is the collecting efficiency of Pt ring (0.37).

Supplemental Figures and Tables.

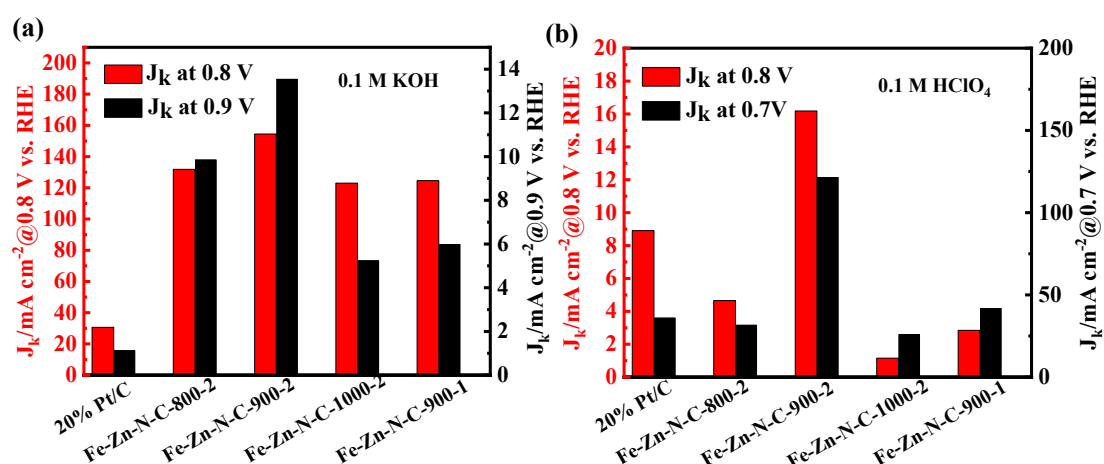


Fig. S1. (a) J_k of catalysts at 0.8 and 0.9 V in 0.1 M KOH; (b) J_k of catalysts at 0.7 and 0.8 V in 0.1 M HClO₄.

Table S1. J_k values of catalysts in 0.1 M KOH and 0.1 M HClO₄.

Catalyst	0.1 M HClO ₄		0.1 M KOH	
	$J_k/\text{mA cm}^{-2}@0.7\text{ V}$	$J_k/\text{mA cm}^{-2}@0.8\text{ V}$	$J_k/\text{mA cm}^{-2}@0.8\text{ V}$	$J_k/\text{mA cm}^{-2}@0.9\text{ V}$
Fe-Zn-N-C-800-2	31.50	4.65	131.86	9.84
Fe-Zn-N-C-900-2	121.30	16.18	154.46	13.53
Fe-Zn-N-C-1000-2	25.84	1.15	123.01	5.23
Fe-Zn-N-C-900-1	41.65	2.84	124.60	5.98
20% Pt/C	35.85	8.91	30.62	1.12

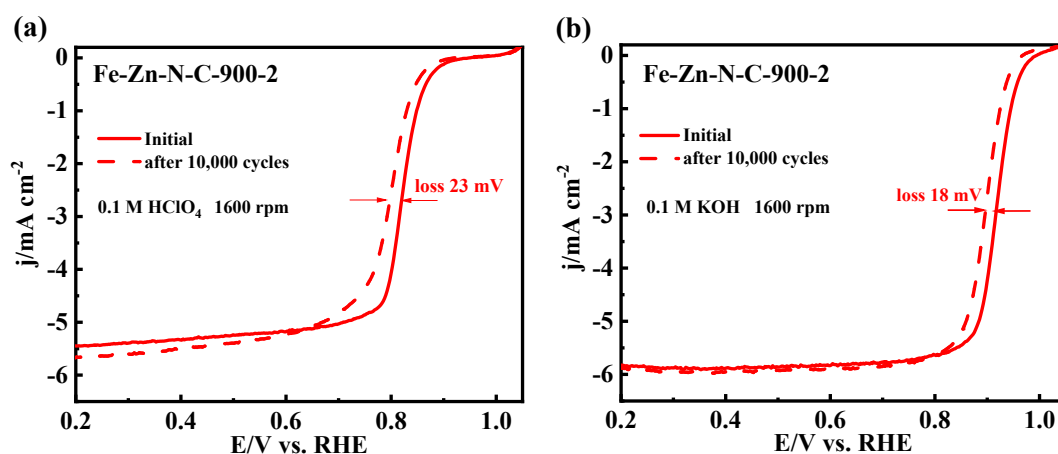


Fig. S2. LSV curves of Fe-Zn-N-C-900-2 in (a) 0.1 M HClO₄ and (b) 0.1 M KOH before and after durability test (1600 rpm and 10 mV s⁻¹).

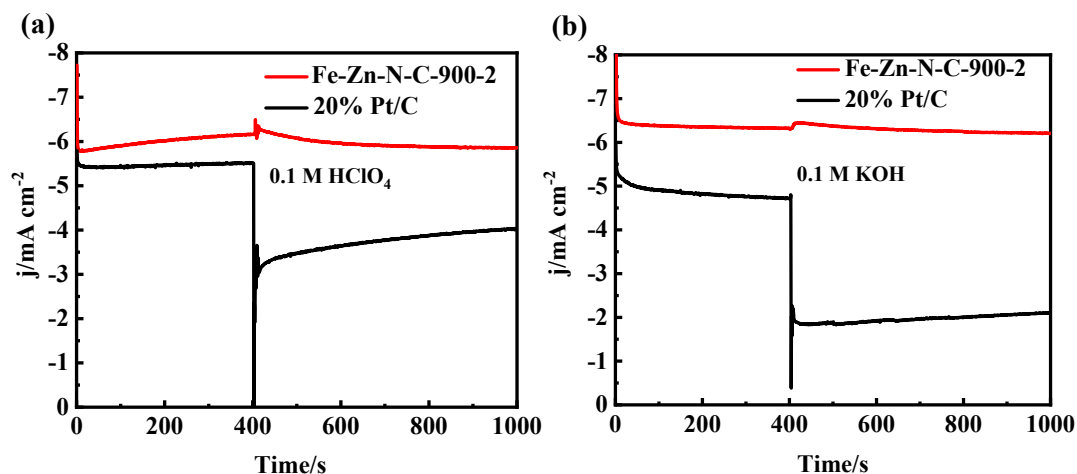


Fig. S3. Methanol tolerance of Fe-Zn-N-C-900-2 and Pt/C in (a) 0.1M HClO₄ and (b) 0.1M KOH.

Table S2. ORR performance comparison for typical non-precious-metal catalysts.

Catalyst	$E_{1/2}/V$ vs. RHE		Ref.
	In acidic media	In alkaline media	
Fe-Zn-N-C-900-2	0.819	0.918	This work
Fe-Fe ₃ C@Fe-N-C	0.79	0.88	1
Fe-ISAs/CN	0.773	0.900	2
Zn-N-C-1	0.746	0.873	3
Fe _{SA} -N-C	0.776	0.891	4
Zn/CoN-C	0.796	0.861	5
m-FeSNC	-	0.904	6
ZIF ⁷ -FA-p	0.81	-	7
Fe@C-Fe-N-C	0.730	0.899	8
SA-Fe-HPC	0.81	0.89	9
SA-Fe/NG	0.80	0.88	10
Fe ₃ N-PCNs	-	0.87	11
Fe/Fe ₃ C ₂ @N-C	0.66	0.85	12
Zn/CoN-C	0.796	0.861	13
Fe ₃ N-HPCC	0.76	0.898	14
FeN _x /GM	0.80	-	15
p-Fe-NCNF	0.74	0.82	16

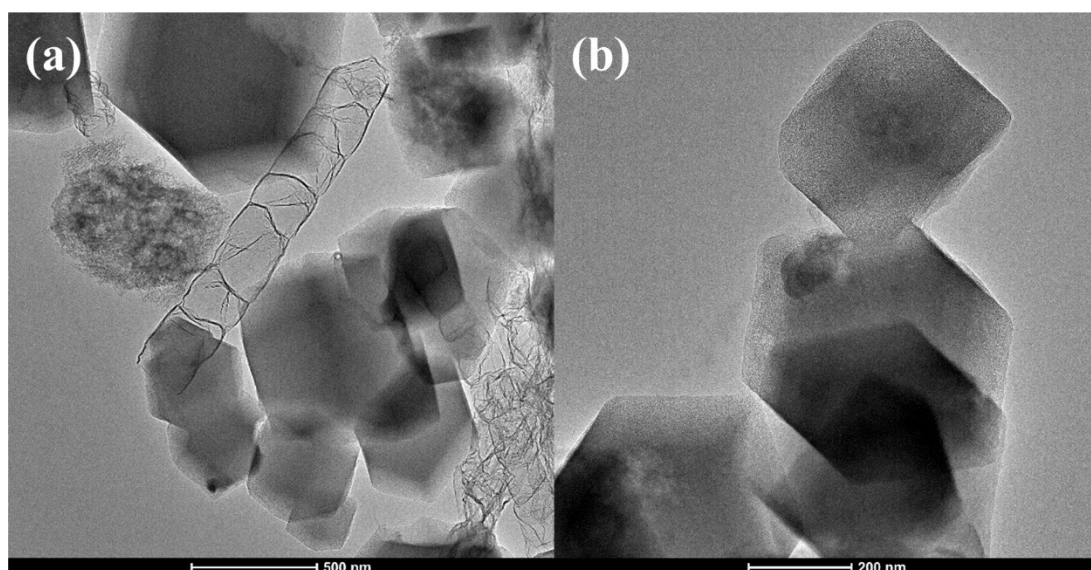


Fig. S4. TEM images of Fe-Zn-N-C-900-2 (a) and Fe-Zn-N-C-900-1 (b).

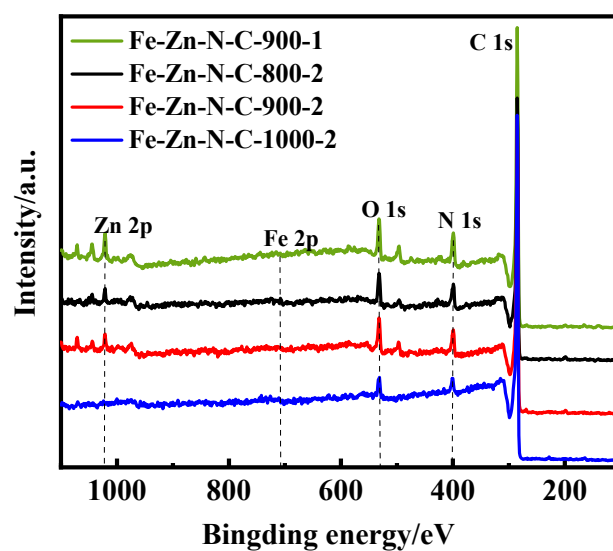


Fig. S5. XPS spectra of Fe-Zn-N-C samples.

Table S3. The composition of Fe-Zn-N-C samples.

Sample	C/at. %	N/at. %	O/at. %	Fe/at. %	Zn/at. %
Fe- Zn -N-C-900-1	85.40	7.94	5.58	0.32	0.76
Fe-Zn-N-C-800-2	85.74	7.25	5.67	0.74	0.60
Fe-Zn-N-C-900-2	86.70	6.78	5.43	0.59	0.51
Fe-Zn-N-C-1000-2	92.78	3.31	3.39	0.38	0.14

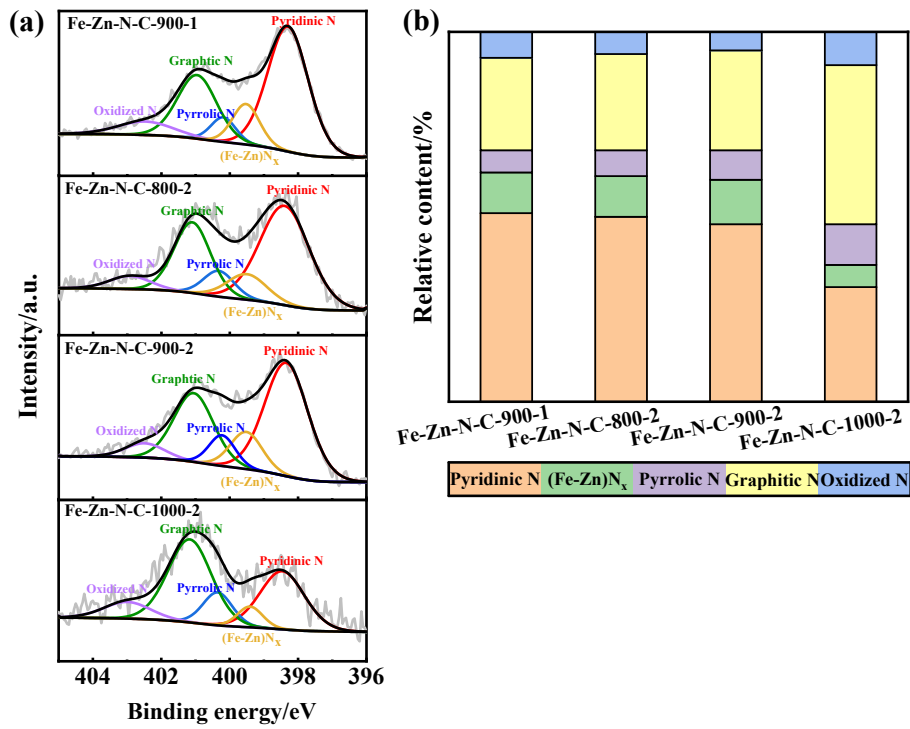


Fig. S6. (a) High-resolution N1s XPS spectra of Fe-Zn-N-C samples and (b) the relative contents of the deconvoluted peak areas of N1s XPS spectra.

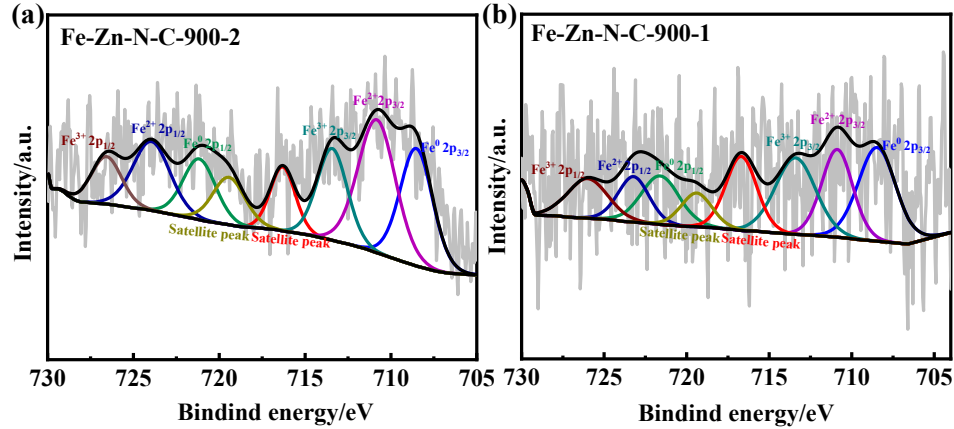


Fig. S7. High-resolution Fe 2p XPS spectra of (a) Fe-Zn-N-C-900-2 and (b) Fe-Zn-N-C-900-1 samples.

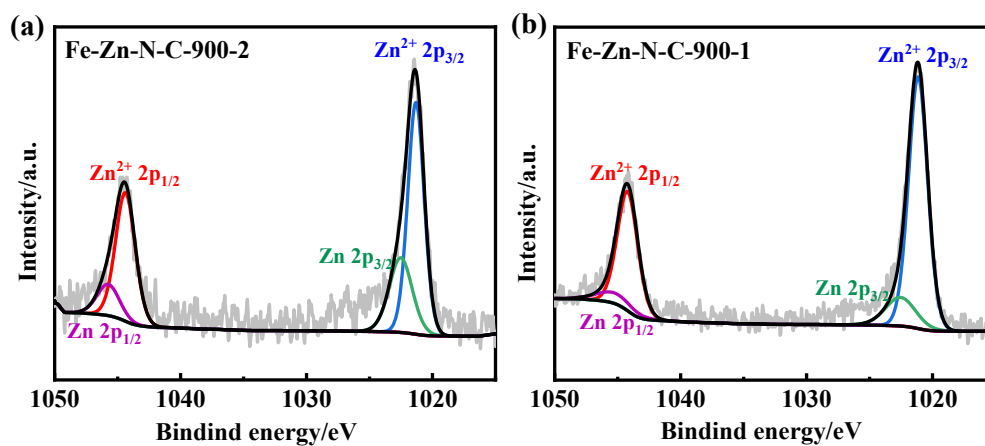


Fig. S8. High-resolution Zn 2p XPS spectra of (a) Fe-Zn-N-C-900-2 and (b) Fe-Zn-N-C-900-1 samples.

Table S4. Specific surface area and pore volume values of Fe-Zn-N-C samples.

Samples	$S_{\text{BET}}/\text{m}^2 \text{g}^{-1}$	$V_{\text{total pore}}/\text{cm}^3 \text{g}^{-1}$	$V_{\text{micro}}/\text{cm}^3 \text{g}^{-1}$	$V_{\text{meso/macro}}/\text{cm}^3 \text{g}^{-1}$
Fe-Zn-N-C-800-2	1393	0.844	0.355	0.489
Fe-Zn-N-C-900-2	1303	0.869	0.323	0.546
Fe-Zn-N-C-1000-2	1211	1.018	0.264	0.754
Fe-Zn-N-C-900-1	1257	0.744	0.328	0.416

References

1. H. Wang, F. X. Yin, N. Liu, R. H. Kou, X. B. He, C. J. Sun, B. H. Chen, D. J. Liu and H. Q. Yin, *Adv. Funct. Mater.*, 2019, **29**, 1-11.
2. Y. Chen, S. Ji, Y. Wang, J. Dong, W. Chen, Z. Li, R. Shen, L. Zheng, Z. Zhuang, D. Wang and Y. Li, *Angew. Chem. Int. Ed.*, 2017, **56**, 6937-6941.
3. J. Li, S. Chen, N. Yang, M. Deng, S. Ibraheem, J. Deng, J. Li, L. Li and Z. Wei, *Angew. Chem. Int. Ed.*, 2019, **58**, 7035-7036.
4. L. Jiao, G. Wan, R. Zhang, H. Zhou, S.-H. Yu and H.-L. Jiang, *Angew. Chem. Int. Ed.*, 2018, **57**, 8525-8529.
5. Z. Lu, B. Wang, Y. Hu, W. Liu, Y. Zhao, R. Yang, Z. Li, J. Luo, B. Chi, Z. Jiang, M. Li, S. Mu, S. Liao, J. Zhang and X. Sun, *Angew. Chem. Int. Ed.*, 2019, **58**, 2622-2626.
6. Z. Guan, X. Zhang, W. Chen, J. Pei, D. Liu, Y. Xue, W. Zhu and Z. Zhuang, *Chem. Commun.*, 2018, **54**, 12073-12076.
7. C. Zhang, Y. C. Wang, B. An, R. Huang, C. Wang, Z. Zhou and W. Lin, *Adv. Mater.*, 2017, **29**, 1-7.
8. W.-J. Jiang, L. Gu, L. Li, Y. Zhang, X. Zhang, L.-J. Zhang, J.-Q. Wang, J.-S. Hu, Z. Wei and L.-J. Wan, *J. Am. Chem. Soc.*, 2016, **138**, 3570-3578.
9. Z. Zhang, J. Sun, F. Wang and L. Dai, *Angew. Chem. Int. Ed.*, 2018, **57**, 9038-9043.
10. L. Yang, D. Cheng, H. Xu, X. Zeng, X. Wan, J. Shui, Z. Xiang and D. Cao, *Proc. Natl. Acad. Sci. USA*, 2018, **115**, 6626-6631.
11. P. Du, F.-X. Ma, F. Lyu, K. He, Z. Li, J. Lu and Y. Y. Li, *Chem. Commun.*, 2019, **55**, 5789-5792.
12. L. Song, T. Wang, L. Li, C. Wu and J. He, *Appl. Catal. B-Environ.*, 2019, **244**, 197-205.
13. Z. Lu, B. Wang, Y. Hu, W. Liu, Y. Zhao, R. Yang, Z. Li, J. Luo, B. Chi, Z. Jiang, M. Li, S. Mu, S. Liao, J. Zhang and X. Sun, *Angew. Chem. Int. Ed.*, 2019, **131**, 2648-2652.
14. Z. Guo, Z. Zhang, Z. Li, M. Dou and F. Wang, *Nano Energy*, 2019, **57**, 108-117.
15. X. Fu, N. Li, B. Ren, G. Jiang, Y. Liu, F. M. Hassan, D. Su, J. Zhu, L. Yang, Z. Bai, Z. P. Cano, A. Yu and Z. Chen, *Adv. Energy Mater.*, 2019, **0**, 1803737.
16. B.-C. Hu, Z.-Y. Wu, S.-Q. Chu, H.-W. Zhu, H.-W. Liang, J. Zhang and S.-H. Yu, *Energ. Environ. Sci.*, 2018, **11**, 2208-2215.